IOP Conf. Series: Materials Science and Engineering **207** (2017) 012084 doi:10.1088/1757-899X/207/1/012084

First-principles study of electronic, mechanical and optical properties of mixed valence SmB_6

Lihua Xiao [1, 2, 3*], Yuchang Su[2] Ping Peng[4] and Dongsheng Tang[1]

[1]College of Physics and Information Science, Hunan Normal University, Changsha, China
[2]School of Materials Science and Engineering, Central South University, Changsha, China
[3]School of Materials and Metallurgical Engineering, Guizhou Institute of Technology, Guiyang, China
[4]School of Materials Science and Engineering, Hunan University, Changsha, China

*Corresponding author e-mail: xiaolihua@git.edu.cn, dstang@hunnu.edu.cn

Abstract. The mechanical and optical properties, electronic structure, and theoretical hardness of mixed valence SmB_6 are calculated from first principles using density functional theory. The calculated results are in excellent agreement with previously reported experiments and theory. The band structures of SmB_6 reveal that this material has the qualities of a semiconductor with a minimum gap. The elastic constants, bulk modulus, shear modulus and Young's moduli of SmB_6 are obtained. The calculated results indicate that SmB_6 is a brittle material. The calculated theoretical hardness is 24.00 GPa. The optical properties of SmB6 are discussed in detail. It is shown that SmB_6 absorbs in the near infrared and visible light range. Therefore, SmB_6 has the potential to be used as a heat-absorbing coating in order to shield objects from solar heat radiation.

1. Introduction

Rare earth hexaborides (RB_6) have been widely studied because of their low densities, low thermal expansion coefficients, high melting points, high harnesses, high chemical stabilities, superconductivity capabilities, [1-4] magnetic properties,[5,6] high efficiency thermionic emission abilities,[7–10] narrow band gap semiconductivities,[11] and others.[12,13] Recently, these materials have been used in transparent heat-insulating windows[14-17] by taking advantage of their strong near-infrared radiation absorption and their high visible light transmittance that arise from the free electron plasmatic behaviors. The unusual properties of rare earth hexaborides are ascribed to the interaction of the 5*d* and 4*f* electrons of R with the 2*p* conduction electrons of B. These interactions seem to play an important role in determining the electrical, optical and mechanical properties of these materials.

The mixed valence compound SmB_6 belongs to a family of extremely hard and stable metal hexaborides. SmB_6 has been well studied because of its topological Kondo insulator properties which have intrigued physicists for many years. There have been significant theoretical and experimental

Efforts to understand the physical properties of SmB_6. Recent theoretical predictions have suggested that the mixed valence compound SmB_6 exhibits a topological Kondo insulator phase.[18-21]

Researchers have experimentally probed the topological Kondo insulator properties of SmB_6 by performing transport measurements,[22-25] torque magnetometer measurements,[26] neutron measurements,[27,28] various angle-resolved photoemission spectroscopy,[29-35] and scanning tunneling microscopy measurements.[36-38] The mechanical and optical properties of SmB_6 are very important owing to its applications as photoelectric functional material. At present, only a few reports have performed to investigate the mechanical and optical properties for SmB_6 and the results also provided some useful information. [16, 17, 39-42] However, the systematical information of mechanical and optical properties is still lack, which hinders the better understandings and applications of SmB_6. A systematic compilation of these properties is crucial for further material design and better understanding how to utilize SmB_6. Therefore, a systematic study of the electronic, mechanical and optical properties of SmB_6 must be performed to provide supplements to these shortages using the present first principles calculations.

In the present work, we investigated the electronic, mechanical and optical properties of SmB_6 using the first-principles calculations. This paper is organized as follows. First, the computational details based on first-principles calculations are depicted. Then, the structural properties, electronic structures, elastic constants, mechanical and optical properties for SmB_6 are presented. Finally, the conclusions of the present work are given.

2. Computational details

SmB_6 is ferromagnetic at low temperatures. Therefore, the spin polarized calculations, including spin-orbit coupling, were performed using density-functional theory (DFT) [43] as implemented in the Cambridge sequential total energy package (CASTEP) code. [44] The Vanderbilt-type ultra-soft pseudopotential was used to describe the interactions between ions and electrons. The exchange-correlation energy was described by a generalized gradient approximation (GGA) of the Pardew-Burke-Ernzerhof (PBE) [45] parameterization. The ultra-soft pseudo-potentials in this work were performed with $4f^6 5p^6 6s^2$ and $2s^2 2p^1$ valence-electron configurations for Sm and B atoms, respectively. The change of total energy during the optimization was converged to 1×10^{-6} eV and the forces per atom were reduced to 0.02 eV/Å. The Brayden-Fletcher-Goldfarb-Shannon (BFGS) algorithm was applied to relax the crystal structure to reach the ground state where both the cell parameters and the fractional coordinates of the atoms were simultaneously optimized. Brillouin zone (BZ) integrations were performed using Monk horst-Pack [46] *k*-point meshed. The *k* point separation in the Brillouin zone of the reciprocal space was $10\times10\times10$ for SmB_6. The cut-off energy for plane wave expansions was determined to be 400 eV. The separation of the reciprocal space was around 0.01 $Å^{-1}$ and the self-consistent field (SCF) tolerance was set to 5.0×10^{-7} eV/atom. The tolerance for elastic constants was set to within 1.0×10^{-6} eV/atom, a maximum force within 0.002 eV/ Å, and a maximum strain amplitude within 0.003 GPa.

3. Results and discussion

3.1. Structural properties and elastic constants

At ambient pressure, SmB_6 crystallizes in the cubic CsCl lattice structure and with a P*m*3*m* space group in which the hexaboride cluster (B_6) form a three-dimensional network with the octahedral structure. The Sm atom and B_6 octahedron occupy the site of cesium and chlorine, respectively. The crystal structure is shown in Fig. 1. Sm is located at the Wyckoff position 1*a* (0, 0, 0) and the B atoms at the 6f (1/2, 1/2, *z*) site (Fig. 1a). The boron-framework consists of octahedral B_6 groups joined together as shown in Fig. 1b. The framework has two kinds of boron-boron bonds where $B\text{-}B_{in}$ is on the edge of the octahedron and $B\text{-}B_{out}$ is between the octahedral. The $B\text{-}B_{in}$ distance is larger than the $B\text{-}B_{out}$ distance in SmB_6, which shows that the large octahedron keeps a large distance between neighboring Sm atoms.

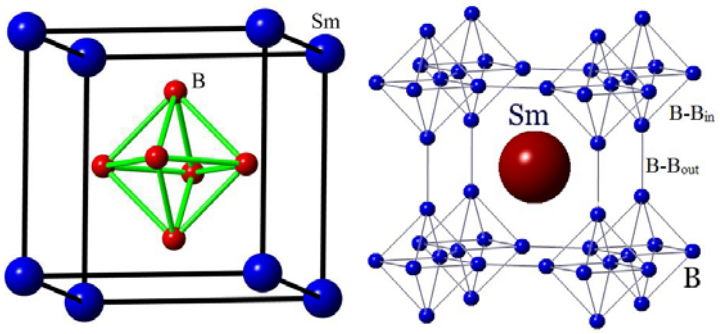

Figure 1. The crystal structure of SmB6. (a) Primitive cell and (b) Occupied sites of Sm atoms'–Bin and B–Bout are the inter-octahedral and intra-octahedral boron bond lengths, respectively.

The calculated lattice parameter (a_0) and internal parameter (z) of SmB_6 are listed in Table 1 along with available experimental and theoretical values. The calculated parameters are slightly larger than the experimental ones due to the inherent nature of the GGA approximation. The results of our calculations are in good agreement with previous experimental and theoretical data.

Table 1. Calculated and experimental structural parameters and the plasma energy (ωp) of SmB_6

	a_0(Å)	z	B-B_{in} (Å)	B-B_{out} (Å)	M-B(Å)	ω_p(eV)
Calc.[a]	4.1704	0.2018	1.7588	1.6831		1.34
	4.133[42]					
Expt.	4.1346[47]	0.2018[47]	1.7438[47]	1.6688[47]	3.0381[47]	
	4.131[39]					
	4.133[48]					

[a]This work.

In order to study the mechanical properties of SmB_6, its Elastic constant C_{ij}, bulk modulus B, shear modulus G, Young's modulus E and Poisson's ratio σ were calculated. The experimental data from the literature are shown in Table 2. For the cubic crystal, the mechanical stability leads to restrictions on the elastic constants as follows: $C_{44} > 0$ $C_{11} > C_{12}$, $C_{11} + 2C_{12} > 0$. The elastic constant C_{11} represents the elasticity in length while C_{12} and C_{44} are related to the elasticity in shape. Table 2 shows that the elastic constants of SmB_6 satisfy all of these criteria. It is important to note that the calculated elastic properties of SmB_6 agree well with the available experimental data. [41] Unfortunately, to our knowledge, there are no theoretical data in which to compare our elastic constants of SmB_6. Therefore, our results were compared to the experimental and theoretical elastic constants of other hexaborides, such as RB_6 (R=Y, La, Eu and Gd) [49] and MB_6 (M=Ca, Sr and Ba). [50] When comparing to these data, our calculated results are reasonable. From the ratio of B/G and Poisson's ratio σ, one can judge whether a material is ductile or brittle. The threshold of B/G and Poisson's ratio σ was found to be around 1.75 and 0.26, respectively. When $B/G > 1.75$ and $\sigma > 0.26$, the material behaves in a ductile manner, whereas it behaves in a brittle manner with values lower than 1.75 and 0.26, respectively. It is obvious from Table 2 that SmB_6 is brittle in nature.

Table 2. Elastic constants Cij(GPa), bulk modulus B(GPa), shear modulus G(GPa),Young's modulus E(GPa), B/G, and Poisson's ratio σ of SmB_6

	C_{11}	C_{12}	C_{44}	B	G_V	G_R	G	B/G	E	σ
Calc.[a]	415.89	9.88	75.69	145.22	126.61	101.03	113.82	1.28	415.43	0.023
	465[40]	29[40]	56[40]	174.1[40]						
Expt.	417[41]	-67[41]	78[41]	166.0[41]						

3.2. Electronic structure, magnetic properties and theoretical hardness

The energy band of the mixed valence compound SmB_6 was investigated to compare the exchange interaction. The energy band corresponding to the spin-up and spin-down split apart is due to the exchange coupling between the electrons. The spin energy band structures of SmB_6 are show in Fig. 2. The low energy band structures of SmB_6 have characteristics of semiconductors in that they have with a minimum gap of about 130 meV along the X-R direction in the majority spins (spin up) states and about 200 meV in the minority spins (spin down) states. The Sm-4*f* orbitals form narrow bands under the Fermi level in the majority spins (spin up) states. Our calculated energy band structures are in good agreement with results produced by the LDA + Gutzwiller method of Lu *et al* [51] and with the experimental results from transport and optical measurements which revealed the formation of a small gap only at temperatures under 50 K. [52-54]

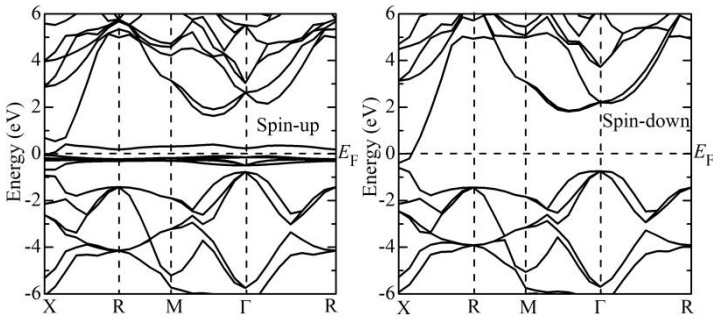

Figure 2. The spin energy band structure of SmB_6

The origin of the magnetic behaviors of SmB_6 was studied by calculating and analyzing the spin-projected total and partial density of states (DOS) for magnetic spin-states (Fig. 3). The spin-projected density of states of SmB_6 consists of four parts. The first part of bands consists of Sm 5*p* and B 2*s*2*p* states (-20 to -12 eV). The second part of bands (-10 to -1 eV) is characterized by B 2*p* states and some amount of Sm 5*s*5*p* states in order to make the distribution of spin-projected total density of states overall symmetric. It is interesting to note that 4*f* states cross the Fermi energy E_F, and hybridize with 5*d* states near the E_F, which is consistent with various experimental results. [55-57] The last group of bands (above E_F) is mainly made up of Sm 5*d*4*f* states. The Sm 5*d* band has a higher energy than La 5*d* in the lanthanum hexaboride due to the mixed valence character of SmB_6. The bottom of the conduction band and the top of the valence band are mainly formed from hybridized Sm 4*f* states and from B 2*p* states; there is also some amount of Sm 5*d* states and B 2*p* states. Figure 3 shows that orbital polarization is negligible for SmB_6.

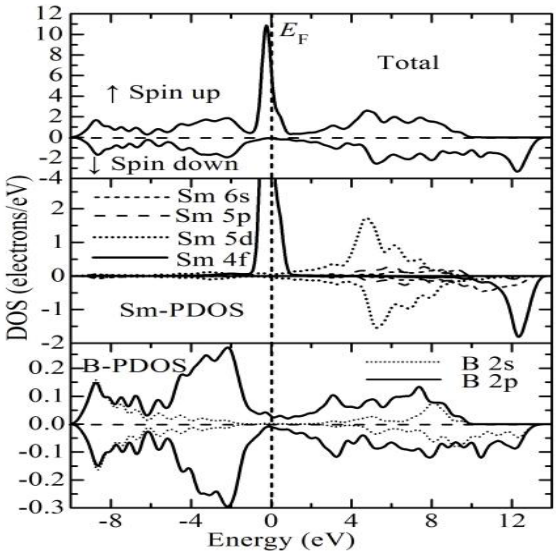

Figure 3. Spin-projected densities of states of SmB6

The Mullikan charge and overlap population are useful in evaluating the covalent, ionic, or metallic nature of bonds in a compound. Therefore, the Mullikan charge population for SmB_6 was calculated in order to better understand bonding in this compound. The Mullikan population results are given in Table 3. The calculated charge transfer from Sm to B is about 2.29 *e*. This value indicated that the bonding behaviour in SmB_6 is a combination of covalent and ionic. The Mullikan charge populations for SmB_6 were also calculated in order to obtain the intrinsic hardness of SmB_6 on the basis of Gao's model.[54] The intrinsic hardness of each chemical bond was calculated using the data in Table 4. Previous work has suggested that the hardness of complex compounds can be expressed as a geometric average of the hardness of all binary systems in the solid. This rule of considering the joint contributions of different bindings was applied to our calculations. [50] The calculated hardness values listed in Table 4 generally agree with previous experimental results. [39]

Table 3. Mullikan charge population of SmB6

Species	*s*	*p*	*d*	f	Total (*e*)	Charge (*e*)
B	0.85	2.53	0.00	0.00	-0.38	
Sm	1.81	5.17	0.81	5.92	13.71	2.29

Table 4. Calculated Mullikan population analysis and hardness (GPa) of SmB6.

	Atom	Charge (e)	Bond	Population	Length (Å)	N^{μ}	Vcell (Å^3)	v^{μ}	H^{μ}	H	$H_{Exp.}$ [39]
SmB_6	Sm_{1a}	2.29	B-B_{in}	0.58	1.6831	3	72.53	4.49	35.12	24.00	17.8±0.065
	B_{6f}	-0.38	B-B_{out}	0.45	1.7587	12		5.13	21.82		

3.3. Optical properties

The optical properties of a solid material are determined by the frequency-dependent dielectric function $\varepsilon(\omega) = \varepsilon_1(\omega) + \varepsilon_2(\omega)$, which characterizes the linear response of the material to an electromagnetic radiation (e.g. Governs the propagation behavior of radiation in a medium). The imaginary part of the dielectric function ε2 (ω) is calculated from the momentum matrix elements between the occupied and unoccupied electronic states. The real part $\varepsilon_1(\omega)$ is derived from the imaginary part $\varepsilon_2(\omega)$ by the Kramers-Kronig transformation. All other optical constants, such as

reflectivity, the absorption value, and the electron energy-loss function value are derived from $\varepsilon_1(\omega)$ and $\varepsilon_2(\omega)$.[58]

The complex dielectric function, reflectivity, the absorption spectrum, and the electron energy-loss function as a function of photon energy are presented in Fig. 4-7. The calculated static dielectric constant $\varepsilon_1(\omega)$ was found to be 36.67. The peaks of the imaginary part of the dielectric function $\varepsilon_2(\omega)$ are related to the electron excitation. These peaks which have a relatively strong intensity are located at 0.47 eV (A), 4.09 eV (B), and 6.98 eV (C). Peak A is ascribed to the transition of the inner electron excitation of Sm 4*f* states. Peak B and peak Care ascribed to the transition between B 2*p* states in the valence bands and Sm 5*d* states in the conduction bands.

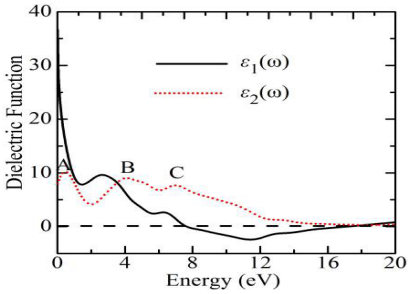

Figure 4. (Color online) Dielectric function of SmB6.

The reflectivity spectra were derived from the calculated dielectric functions for SmB_6 and are shown in Fig. 5. The calculated reflectivity was compared to the experimental data from Kimura *et al*. [59] Evidently, The experimental value shows a large value of reflectivity in the low energy range. Our calculated reflectivity also shows similar characteristics. In addition, the calculated result shows a dip below 1.78 eV in the visible light range. This is in good agreement with the experimental data from Kimura *et al*. (1.8 eV). [60]

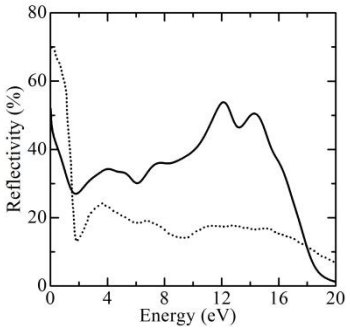

Figure 5. Reflectivity of SmB6. The dotted line stands for experimental data of SmB6. [59]

By analyzing the transmittance profiles of nanoparticle dispersions of rare-earth hexaborides, Takeda et *al.* concluded that hexaboride nanoparticles have potential uses as coatings for solar control windows to shield against solar heating. These results inspired us to study the absorption spectrum of SmB_6. Fig. 6 shows the calculated absorption spectrum of SmB_6. The strong absorption coefficient above 10^5 cm^{-1} occurs in the near infrared and visible light range because it is a metallic compound. The absorption spectrum has a sharp increase of about 3 eV in the high-energy region. Most significantly, there are no significant absorption peaks in the near infrared and visible light ranges. Therefore, we conclude that SmB_6 is a candidate for use in heat-absorbing coatings to shield solar heating.

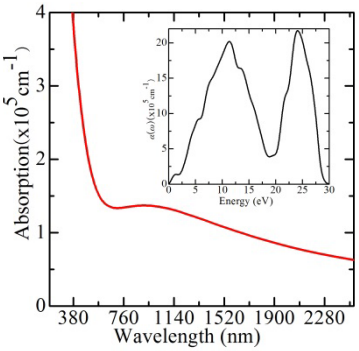

Figure 6. Absorption spectrum of SmB6.

The electron energy-loss function describes the energy loss of electrons that quickly traverse materials. The peak in the low-loss region characterizes the plasma resonance and the peak position corresponds to the relevant plasma frequency ω_p. Fig. 7 shows the calculated electron energy-loss spectrum. According to Kimura *et al.*, [59] the peak at 1.34 eV is derived from the excitation of the plasmon of the conduction electron. Additionally, the peak at 17.4 eV can be attributed to the excitation of the plasmon of the valence band which consists of the boron 2s and 2p bonding states and the $4f_{5/2}$ state of Sm atom. The peak at 28.0 eV shows the transition or excitation from 5p states. By comparing this information with other literature, [16] we conclude that the very weak peak at 1.34 eV, which is the plasma energy $\hbar\omega_p$ of SmB_6, shows a plasma resonance in the low-energy scale. This corresponds to an abrupt descent in reflectivity.

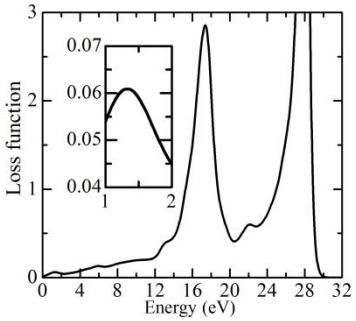

Figure 7. Energy-loss spectrum of SmB6.

4. Conclusion

In summary, first-principles calculations were used to investigate the structural parameters, mechanical properties, electronic structure, theoretical hardness and optical properties of SmB_6. The band structures of SmB_6 showed that this material has properties of a semiconductor (i.e. a minimum gap). The elastic constants, bulk modulus, shear modulus and Young's moduli of SmB_6 were calculated. These results showed that SmB_6 is brittle in nature. A theoretical hardness of 24.00 GPa was calculated. Finally, the dielectric function, reflectivity, absorption spectrum and electron energy-loss spectrum were obtained and discussed in detail. Our calculated reflectivity spectrum is in good agreement with the experimental literature. The absorption spectrum of SmB_6 shows that it has the potential for use as a heat-absorbing coating in order to shield solar radiation. We hope that our calculated results provide the theoretical data that are necessary for further material design and development of applications of the topological Kondo insulator SmB_6.

Acknowledgments
This work was financially supported by the National Natural Science Fund (No. 11574081), Guizhou Province Science and Technology Department-Guizhou Institute of Technology Joint Fund (Guizhou Science and Technology Agency LH [2014] 7357) and the Natural Science Foundation of Guizhou Province (Guizhou Science and Technology Agency J [2014]2086).

References
[1]. Matthias B T, Geballe T H, Andres K, et al. Superconductivity and ant ferromagnetism in boron-rich lattices. Science. 159 (1968).
[2]. Hiebl K, Sienko M J. Chemical control of superconductivity in the hexaborides. Inorg Chem. 19 (1980) 2179-2180.
[3]. Bat'ko I, Bat'kova M, Flachbart K, et al. Electrical resistivity and superconductivity of LaB6 and LuB12. J. Alloys Compd. 217 (1995) L1-L3.
[4]. Schell G, Winter H, Rietschel H, et al. Electronic structure and superconductivity in metal hexaborides. Phys. Rev. B 25 (1982) 1589.
[5]. Shannon J R, Sienko M J. Long-range magnetic interactions in europium hexaborides. Inorg Chem. 11 (1972) 904-906.
[6]. Segawa K, Tomita A, Iwashita K, et al. Electronic and magnetic properties of heavy rare-earth hexaboride single crystals. J Magn Magn Mater. 104 (1992) 1233-1234.
[7]. Zhang H, Zhang Q, Zhao G, et al. Single-crystalline GdB6 nanowire field emitters. J. Am. Chem. Soc. 127 (2005) 13120-13121.
[8]. Zhang H, Tang J, Zhang Q, et al. Field emission of electrons from single LaB6 nanowires. Adv. Mater. 18 (2006) 87-91.
[9]. Xu J, Hou G, Li H, et al. Fabrication of vertically aligned single-crystalline lanthanum hexaboride nanowire arrays and investigation of their field emission. NPG Asia Mater. 5 (2013) e53.
[10]. Xu J, Hou G, Mori T, et al. Excellent Field-Emission Performances of Neodymium Hexaboride (NdB6) Nano needles with Ultra-Low Work Functions. Adv. Funct. Mater. 23 (2013) 5038-5048.
[11]. Ishii M, Aono M, Muranaka S, et al. Raman spectra of metallic and semiconducting metal hexaborides (MB6). Solid State Commun. 20 (1976) 437-440.
[12]. Kerley E L, Hanson C D, Russell D H. Lanthanum hexaboride electron emitter for electron impact and electron-induced dissociation Fourier transform ion cyclotron resonance spectrometry. Anal. Chem. 62 (1990) 409-411.
[13]. Takeda M, Fukuda T, Domingo F, et al. Thermoelectric properties of some metal borides. J Solid State Chem. 177 (2004) 471-475.
[14]. Schelm S, Smith G B. Dilute LaB6 nanoparticles in polymer as optimized clear solar control glazing. Appl. Phys. Lett. 82 (2003) 4346-4348.
[15]. Takeda H, Kuno H, Adachi K. Solar Control Dispersions and Coatings with Rare-Earth Hexaboride Nanoparticles. J. Am. Chem. Soc. 91 (2008) 2897-2902.
[16]. Xiao L, Su Y, Zhou X, et al. Origins of high visible light transparency and solar heat-shielding performance in LaB6. Appl. Phys. Lett. 101 (2012) 041913.
[17]. Xiao L, Su Y, Chen H, et al. Study on the electronic structure and the optical performance of YB6 by the first-principles calculations. AIP Advances, 1 (2012) 022140.
[18]. Dzero M, Sun K, Galitski V, et al. Topological Kondo insulators. Phys. Rev. Lett. 104 (2010) 106408.
[19]. Dzero M, Sun K, Coleman P, et al. Theory of topological Kondo insulators. Phys. Rev. B 85 (2012) 045130.
[20]. Miyazaki H, Hajiri T, Ito T, et al. Momentum-dependent hybridization gap and dispersive in-gap state of the Kondo semiconductor SmB6. Phys. Rev. B 86 (2012) 075105.
[21]. Lu F, Zhao J Z, Weng H, et al. Correlated topological insulators with mixed valence. Phys. Rev.

Lett. 110 (2013) 096401.
[22]. Wolgast S, et al. Low temperature surface conduction in the Kondo insulator SmB6. Phys. Rev. B 88 (2013) 180405(R).
[23]. Kim D J, et al. Surface hall effect and nonlocal transport in SmB6: evidence for surface conduction. Sci. Rep. 3 (2013) 3150.
[24]. Kim D J, Xia J. et al. Topological surface state in the Kondo insulator samarium hexaboride. Nat. Mater. 13 (2014) 466.
[25]. Zhang X H. et al. Hybridization, inter-ion correlation, and surface states in the Kondo insulator SmB6. Phys. Rev. X 3 (2013) 011011.
[26]. Li G, Xiang Z, Yu F, et al. Quantum oscillations in Kondo Insulator SmB6 . arXiv preprint arXiv:1306 (2013) 5221.
[27]. Fuhrman W T, Leiner J, Nikolić P, et al. Spin-exciton and topology in SmB6. arXiv preprint arXiv:1407 (2013) 2647.
[28]. Fuhrman W T, Leiner J, Nikolić P, et al. Interaction Driven Subgap Spin Exciton in the Kondo Insulator SmB6. Phys. Rev. Lett. 114 (2015) 036401.
[29]. Jiang J, Li S, Zhang T, et al. Observation of possible topological in-gap surface states in the Kondo insulator SmB6 by photoemission. Nat. Commun. 4 (2013) 3010.
[30]. Neupane M, Alidoust N, Xu S Y, et al. Surface electronic structure of the topological Kondo-insulator candidate correlated electron system SmB6. Nat. Commun. 4, (2013) 2991.
[31]. Zhu Z H, Nicolaou A, Levy G, et al. Polarity-driven surface metallicity in SmB6. Phys. Rev. Lett. 111 (2013) 216402.
[32]. Xu N, Shi X, Biswas P K, et al. Surface and bulk electronic structure of the strongly correlated system SmB6 and implications for a topological Kondo insulator. Phys. Rev. B 88 (2013) 121102(R).
[33]. Frantzeskakis E, de Jong N, Zwartsenberg B, et al. Kondo hybridization and the origin of metallic states at the (001) surface of SmB6. Phys. Rev. X 3 (2013) 041024.
[34]. Xu N, Biswas P K, Dil J H, et al. Direct observation of the spin texture in SmB6 as evidence of the topological Kondo insulator. Nat. Commun. 5 (2014) 4566.
[35]. Xu N, Matt C E, Pomjakushina E, et al. Exotic Kondo crossover in a wide temperature region in the topological Kondo insulator SmB6 revealed by high-resolution ARPES. Phys. Rev. B 90 (2014) 085148.
[36]. Ruan W, Ye C, Guo M, et al. Emergence of a Coherent In-Gap State in the SmB6 Kondo Insulator Revealed by Scanning Tunneling Spectroscopy. Phys. Rev. Lett. 112 (2014) 136401.
[37]. Yee M M, He Y, Soumyanarayanan A, et al. Imaging the Kondo insulating gap on SmB6. arXiv preprint arXiv:1308 (2013) 1085
[38]. Rößler S, Jang T H, Kim D J, et al. Hybridization gap and Fano resonance in SmB6. Proc Natl Acad Sci. 111 (2014) 4798-4802.
[39]. Futamoto M, Aita T, Kawabe U. Microhardness of hexaboride single crystals. Mater Res Bull. 14 (1979) 1329-1334.
[40]. Jie D, Tong Z, Li Z, et al. Elastic properties and electronic structures of lanthanide hexaborides. Chin. Phys. B. 2015, 24(9): 096201.
[41]. Smith H G, Dolling G, Kunii S, et al. Experimental study of lattice dynamics in LaB6 and YbB6. Solid State Commun. 53 (1985) 15-19.
[42]. Singh N, Saini S M, Nautiyal T, et al. Electronic structure and optical properties of rare earth hexaborides RB6 (R= La, Ce, Pr, Nd, Sm, Eu, Gd). J. Phys.: Condens. Matter 19 (2007) 346226.
[43]. Kohn W, Sham L J. Self-consistent equations including exchange and correlation effects. Phys. Rev. 140 (1965) 1133.
[44]. Segall M D, Lindan P J D, Probert M J, et al. First-principles simulation: ideas, illustrations and the CASTEP code. J. Phys. Condens. Matter 14 (2002) 2717.

[45]. Perdew J P, Burke K, Wang Y. Generalized gradient approximation for the exchange-correlation hole of a many-electron system. Phys. Rev. B 54 (1996) 16533.
[46]. Monkhorst H J, Pack J D. Special points for Brillouin-zone integrations. Phys. Rev. B 13 (1976) 5188.
[47]. Funahashi S, Tanaka K, Iga F. X-ray atomic orbital analysis of 4f and 5d electron configuration of SmB6 at 100, 165, 230 and 298 K. Acta Crystallogr., Sect. B: Struct. Sci 66 (2010) 292-306.
[48]. Zhang M, Jia Y, Xu G, et al. Mg-Assisted Autoclave Synthesis of RB6 (R= Sm, Eu, Gd, and Tb) Submicron Cubes and SmB6 Submicron Rods. Eur J Inorga Chem. 2010 (2010) 1289-1294.
[49]. Grechnev G E, Baranovskiy A E, Fil V D, et al. Electronic structure and bulk properties of MB6 and MB12 borides. Low Temp Phys 34 (2008) 921.
[50]. Huang B, Duan Y H, Sun Y, et al. Electronic structures, mechanical and thermodynamic properties of cubic alkaline-earth hexaborides from first principles calculations. J. Alloys Compd. 635 (2015) 213-224.
[51]. Menth A, Buehler E, Geballe T. Magnetic and semiconducting properties of SmB6. Phys. Rev. Lett. 22 (1969) 295–297.
[52]. Allen J, Batlogg B, Wachter P. Large low temperature Hall effect and resistivity in mixed valent SmB6. Phys. Rev. B 20 (1979) 4807–4813.
[53]. Cooley J, Aronson M, Fisk Z, et al. SmB6: Kondo insulator or exotic metal? Phys. Rev. Lett. 74 (1995) 1629.
[54]. Gao F. Theoretical model of intrinsic hardness. Phys. Rev. B 73 (2006) 132104.
[55]. Chazalviel J N, Campagna M, Wertheim G K, et al. Study of valence mixing in SmB6 by x-ray photoelectron spectroscopy. Phys. Rev. B 14(1976) 4586.
[56]. Allen J W, Johansson L I, Lindau I, et al. Surface mixed valence in Sm and SmB6. Phys. Rev. B 21(1980)1335.
[57]. Beaurepaire E, Kappler J P and Krill G. X-ray-absorption near-edge structure study in mixed-valent samarium systems. Phys. Rev. B 41(1990) 6768.
[58]. Li C, Wang B, Li Y, et al. First-principles study of electronic structure, mechanical and optical properties of V4AlC3. J. Phys. D: Appl. Phys. 42 (2009) 065407.
[59]. Kimura S, Nanba T, Tomikawa M, et al. Electronic structure of rare-earth hexaborides. Phys. Rev. B 46 (1992) 12196.
[60]. Kimura S, Nanba T, Kunii S, et al. Interband optical spectra of rare-earth hexaborides. J Phys Soc Jpn. 59 (1990) 3388-3392.